

# Realization of a Quantum Simulator Based Oracle Machine for Solving Quantum Optimal Control Problem

Jun Li,<sup>1,\*</sup> Xiaodong Yang,<sup>2</sup> Xinhua Peng,<sup>2,3,†</sup> and Chang-Pu Sun<sup>1</sup>

<sup>1</sup>*Beijing Computational Science Research Center, Beijing 100084, China*

<sup>2</sup>*Hefei National Laboratory for Physical Sciences at Microscale and Department of Modern Physics, University of Science and Technology of China, Hefei, Anhui 230026, China*

<sup>3</sup>*Synergetic Innovation Centre of Quantum Information & Quantum Physics, University of Science and Technology of China, Hefei, Anhui 230026, China*

A central challenge in quantum computing is to identify more computational problems for which utilization of quantum resources can offer significant speedup. Here, we construct a quantum simulator based quantum oracle machine to tackle the quantum optimal control problem. We show that the most computationally demanding part of gradient ascent pulse engineering, namely computing the fidelity and gradient for a control input, can be accomplished by the process of evolution and measurement on a quantum simulator. The quantum simulator realizes an oracle function of yielding the desired information for gradient iteration. By posing queries to and receiving messages from the oracle, classical computing devices update the control parameters until an optimum is achieved. To demonstrate the scheme in experiment, we use a nine-spin nuclear magnetic resonance system, on which we have succeeded in preparing a seven-correlated quantum state without involving classical computation of the large Hilbert space evolution.

PACS numbers: 03.67.Lx, 76.60.-k, 03.65.Yz

Past decades have seen enormous progress in exploring the possible ways of using quantum resources to speed up computation [1]. Although universal quantum computation is in principle possible, technical challenges abound that the fabrication of a real quantum computer is still a long way off [2]. Alternatively, special-purpose quantum simulators, whose implementations are less stringent, are likely to appear in the near future [3, 4]. Quantum simulators are tunable quantum devices designed to imitate specific quantum systems of interest. Because they dramatically reduce the spatial and temporal resources required compared with their classical counterparts [5], quantum simulators exhibit great potential in providing speedup for certain computational problems and have already found a variety of applications, such as solving linear equations [6, 7], simulating condensed-matter systems [8], calculating molecular properties [9, 10] and certifying untrusted quantum devices [11].

In this letter, we propose a method based on quantum simulation to tackle the quantum optimal control problem. Optimal control has been an extensively studied subject and widely used technique in various quantum control systems [12]. Normally, it is formulated as a variational problem: given a control fitness function  $f$  that judges the performance for any control pulse  $u$ , the task is to find a control  $u^*$  that can optimize the functional  $f(u)$ . Current numerical optimal control techniques face the serious scalability problem as they involve simulating controlled quantum dynamics, which can be infeasible on classical computers for systems of large dimensions [13]. We address this computational challenge by constructing a quantum variant of the gradient ascent pulse engineering (GRAPE) technique [14]. We show that, given a

trusted quantum simulator that efficiently simulates the evolution of the controlled quantum system, then under reasonable conditions this simulator can be used to efficiently estimate both  $f(u)$  and  $\nabla f(u)$ . There are two scenarios that our scheme is valid: (i) to use a universal quantum simulator to find an optimal control solution for other quantum systems; (ii) or to use the controlled system to compute its own optimal control pulse, here the simulator is accordingly the controlled system itself and need not be universal. In either case, the simulator will significantly save memory cost and time cost and thus will enhance the ability of solving the quantum optimal control problem for large-size quantum systems.

Now we briefly outline the running mechanism of our scheme in terms of Turing's *oracle machine* model [15, 16]. Oracle machine is a Turing machine that is given access to an oracle. The oracle can compute some difficult function at a reasonable cost. From querying the oracle, the oracle machine may acquire increased computational power [17]. This model captures the essential features of our scheme. First, the quantum simulator that we employ can be seen as an oracle that computes the function  $u \rightarrow \{f(u), \nabla f(u)\}$ . Second, the oracle and the other part of the computation are classically connected, that is, they transmit classical data. As is illustrated in Fig. 1, the setup combines classical computing devices and quantum experiments together to implement the procedure of optimal control searching.

The proposed scheme is amenable to experimental implementation with current state-of-the-art quantum technology. We experimentally demonstrated quantum simulator assisted state preparation on a nine-spin nuclear magnetic resonance (NMR) system. Our experimental

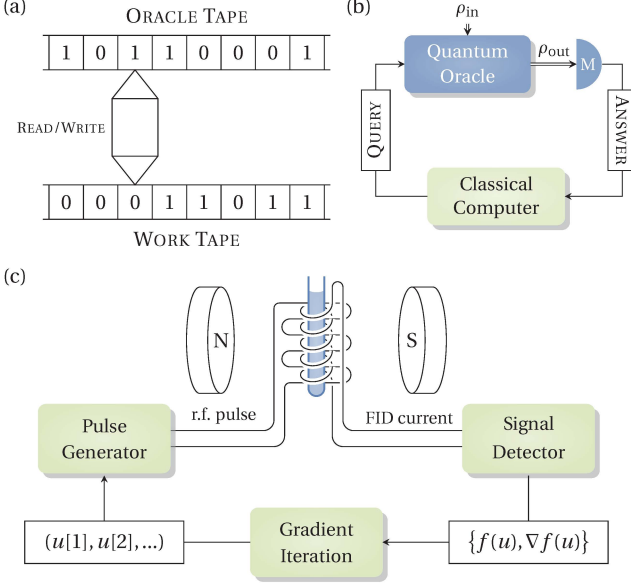


FIG. 1: (a) An oracle machine is a machine that is augmented with an oracle tape such that it may pose questions to the oracle. These questions, are answered consistently by some function. (b) Turing machine with a quantum experimental oracle. Here,  $\rho_{\text{in}}$  is input state,  $\rho_{\text{out}}$  is output state, double-lined arrows signify quantum information, and  $M$  represents quantum measurement. (c) Schematic diagram of an NMR based oracle machine for solving the quantum optimal control problem. The sample consists of an ensemble of spins and is treated as an oracle. Query is encoded in input radio-frequency (r.f.) control pulse and the answer that oracle outputs is extracted by observing the free induction decay (FID).

results show excellent performance of the scheme in obtaining high-quality optimal control solutions.

*Theory.*—To start, we briefly describe the quantum state engineering problem. Consider an  $n$ -spin-1/2 quantum spin system, which evolves under a local Hamiltonian  $H_S = \sum_l^L H_l$ . Here each of the  $L$  terms  $H_l$  acts on a subsystem containing at most a constant number of spins. Such form of Hamiltonian can be efficiently simulated with a quantum simulator [18]. Suppose the system is manipulated with a transverse time-varying magnetic control field  $u(t) = (u_x(t), u_y(t)) : t \in [0, T]$ . Let  $\sigma_x$ ,  $\sigma_y$  and  $\sigma_z$  denote the Pauli operators, then the control Hamiltonian reads  $H_C(t) = \sum_{k=1}^n (u_x(t)\sigma_x^k + u_y(t)\sigma_y^k)$ , in which  $\hbar$  is set as 1 and the gyromagnetic ratios are not written explicitly. The control task is to steer the system between states of interest in the Liouvillian space. Normally a fitness function is needed for judging the control performance. To this end, a set of operators  $\mathcal{P}_n = \{P_k\}_{k=0}^{4^n-1} = \{I, \sigma_x, \sigma_y, \sigma_z\}^{\otimes n}$ , with  $I$  being the  $2 \times 2$  identity, is introduced. It constitutes an orthonormal basis of the state space:  $\text{Tr}(P_k P_j)/2^n = \delta_{kj}$  for  $k, j = 0, \dots, 4^n - 1$ . Any state can thus be represented as a vector with respect to  $\mathcal{P}_n$ . Let the system's starting point be  $\rho_i$  and the target be  $\bar{\rho} = \sum_{s \in S} x_s P_s$  where  $S$

is an index set. Now the state-to-state transfer task is formulated as the quantum optimal control problem [14]:

$$\begin{aligned} \max \quad & f(U(T)\rho_i U(T)^\dagger, \bar{\rho}) = \text{Tr}(U(T)\rho_i U(T)^\dagger \cdot \bar{\rho})/2^n, \\ \text{s.t.} \quad & \dot{U}(t) = -i \left[ H_S + \sum_{k=1}^n (u_x(t)\sigma_x^k + u_y(t)\sigma_y^k) \right] U(t), \end{aligned}$$

where  $U(0) = I^{\otimes n}$  and  $f$ , the fitness function, is expressed as a functional of the input control  $u(t)$  and may possess many local extremums. Except for relatively small systems with two or three qubits [19, 20], analytically deriving globally optimal control for generic  $H_S$  is found to be extremely challenging.

One currently most common numerical approach is to employ the gradient ascent pulse engineering (GRAPE) [14], which works as such: it starts from a designed trial input or just simply a random guess, then iteratively updates the control variables along the gradient direction, and culminates till a local maximum is found. In analyzing the complexity of the optimization procedure, we use the language of oracle model [21, 22]. Suppose that there is an oracle  $\mathcal{O} : u^{(q)} \rightarrow \{f(u^{(q)}), \nabla f(u^{(q)})\}$ , where  $q$  represents that at the  $q$ -th round the algorithm queries the oracle  $\mathcal{O}$  for the values of  $f$  and  $\nabla f$  at point  $u^{(q)}$ . According to the output of  $\mathcal{O}$ , it is decided whether the algorithm proceeds and if so, then at which point the next query should be made. Apparently, the computational labor of the algorithm consists of two parts, i.e., the cost of running oracle and the number of queries in total that are posed to the oracle. The latter characterizes the convergence speed of the algorithm and is referred as query complexity. Although scaling analysis of query complexity is difficult, there are numerical evidences indicating that convergence to an optimal solution is usually fast [23, 24]. Our work concerns the calculation of  $\mathcal{O}$ , which consumes exponential classical resources. To overcome this hurdle, we propose to realize  $\mathcal{O}$  with using a quantum simulator, see Fig. 1(c). Now we assume that we are given a trusted quantum simulator that can efficiently simulate the controlled system evolution. The simulator can be provided by either a universal quantum simulator or the controlled system itself.

Let the pulse  $u(t)$  be divided into  $M$  slices with each time slice being of constant magnitude and fixed length  $\tau = T/M$ . In consideration of memory cost,  $M$  should be polynomially scaled. The  $m$ -th slice control  $u[m]$  generates the propagator

$$U_m = \exp \left\{ -i \left[ H_S + \sum_{k=1}^n (u_x[m]\sigma_x^k + u_y[m]\sigma_y^k) \right] \tau \right\}.$$

For notational brevity let  $U_{m_1}^{m_2}$  denote  $U_{m_2} \cdots U_{m_1+1} U_{m_1}$  where  $m_2 \geq m_1$ . So the final state is  $\rho_f = U_1^M \rho_i U_1^{M\dagger}$ . We hence have the following expression for  $f$

$$f = \text{Tr}(\rho_f \bar{\rho})/2^n = \sum_{s \in S} x_s \text{Tr}(\rho_f P_s)/2^n. \quad (1)$$

It can be readily seen from the equation that, rather than full tomography of final state,  $f$  can be directly measured with  $|S|$  experiments. That is, for the  $s$ -th experiment we first initialize our simulator at  $\rho_i$ , then simulate the controlled evolution according to input query  $u$  and then measure the final state with basis operator  $P_s$ . After this we sum up all the measurement results according to Eq. (1) and hence obtain an estimation of  $f$ .

Next let us see how to compute the  $2M$ -dimensional gradient vector  $g$  of the objective function  $f$ , defined by

$$g[m] = (g_x[m], g_y[m]) = \left( \frac{\partial f}{\partial u_x[m]}, \frac{\partial f}{\partial u_y[m]} \right).$$

To first order approximation, it is evaluated as [14]

$$g_\alpha[m] = \sum_{k=1}^n \text{Tr} \left( -i\tau U_{m+1}^M \left[ \sigma_\alpha^k, U_1^m \rho_i U_1^{m\dagger} \right] U_{m+1}^M \right) / 2^n,$$

here  $\alpha$  is  $x$  or  $y$ . The approximation is good if  $\tau$  is sufficiently small. Note that for any operator  $\rho$ , there is

$$[\sigma_\alpha^k, \rho] = i \left[ \left( \frac{\pi}{2} \right)_\alpha^k \rho \left( \frac{\pi}{2} \right)_\alpha^{k\dagger} - \left( -\frac{\pi}{2} \right)_\alpha^k \rho \left( -\frac{\pi}{2} \right)_\alpha^{k\dagger} \right], \quad (2)$$

in which  $(\pm\pi/2)_\alpha^k$  is the  $\pm\pi/2$  rotation about  $\alpha$  axis on the  $k$ -th qubit. The essential point is that we can compute the commutator by means of local qubit rotations. Substituting the formula into  $g$ ,  $g_\alpha[m]$  equals to

$$\tau \sum_{k=1}^n \text{Tr} \left\{ \left[ U_{m+1}^M \left( \frac{\pi}{2} \right)_\alpha^k U_1^m \rho_i \left( U_{m+1}^M \left( \frac{\pi}{2} \right)_\alpha^k U_1^m \right)^\dagger - U_{m+1}^M \left( -\frac{\pi}{2} \right)_\alpha^k U_1^m \rho_i \left( U_{m+1}^M \left( -\frac{\pi}{2} \right)_\alpha^k U_1^m \right)^\dagger \right] \bar{\rho} \right\} / 2^n.$$

Therefore, to obtain the  $m$ -th component of  $g_\alpha$ , we perform  $2n$  experiments: we (i) sequentially take out an element from the operation set  $\{(\pm\pi/2)_\alpha^k\}_{k=1,\dots,n}$ , and insert it after the  $m$ -th slice evolution; (ii) measure the distances of the final states with respect to  $\bar{\rho}$  and (iii) combine all the measurement results. A quick calculation shows that in each round in total  $4nM|S|$  experiments are needed to perform gradient estimation.

Summarizing the above derivation, we conclude that in total we need to perform  $(4nM + 1)|S|$  experiments on the quantum simulator to estimate  $f$  and  $g$ . It is interesting to seek for instances for which our scheme can be qualitatively advantageous over conventional approaches. Obviously that target states possessing exponential number of nonzero components require also that many measurements to take. This implies that, to ensure the whole process be feasible, we have to restrict consideration to specific kind of target states. An important fact in quantum computing says that, to build up quantum operations out of a small set of elementary gates is

generically inefficient [1]. In other words, there are overwhelmingly many states that are complex in the sense that they take exponential size of quantum circuit to approximate. Therefore, it makes sense if we restrict to relatively less complicated states, for example those which admit sparse representation with respect to some basis, where the basis fulfils the condition that measurement of any its element consumes only polynomial resources. In present setting, we will be interested in  $|S|$ -sparse states under basis  $\mathcal{P}_n$  with  $|S| \ll |\mathcal{P}_n|$ . Despite of the problem simplification, from the practical side they are undoubtedly still difficult tasks at current level of large-system control technology. Sparsity assumption drastically reduces the time cost for physically implementing  $\mathcal{O}$  and in consequence the great chance of our oracle machine model to provide significant speedup.

*Experiment.*—We choose the fully  $^{13}\text{C}$ -labeled crotonic acid as our test system. We demonstrate the idea of using the sample to compute its own optimal control pulse. Experiment is carried on a Bruker Avance III 400 MHz spectrometer at room temperature. Details of the molecular structure are given in Fig. 2(a). The four carbon nuclei plus the five proton nuclei constitute a nine-spin system, in which the methyl protons  $\text{H}_3$ ,  $\text{H}_4$  and  $\text{H}_5$  are chemically and magnetically equivalent and hence are indistinguishable. The system Hamiltonian takes the form:  $H_S = \sum_{k=1}^n \Omega_k \sigma_z^k / 2 + \pi \sum_{k < j} J_{kj} \sigma_z^k \sigma_z^j / 2$ , where  $\Omega_k$  is the precession frequency of the  $k$ -th spin, and  $J_{kj}$  is the coupling between the  $k$ -th and  $j$ -th spin. To describe states of the nuclei, we use deviation density matrices, that is, the traceless part of the density matrices up to an overall scale [25]. Our goal is to create the seven-correlated state  $\bar{\rho} = \sigma_z^1 \sigma_z^2 \sigma_z^3 \sigma_z^5 \sigma_z^7 \sigma_z^8 \sigma_z^9$ , which is the largest multiple-correlated operator that can be directly observed from the spectrum. Observation is made on the methyl carbon  $\text{C}_2$  because all the couplings are adequately resolved. Our experiment scheme is divided into two parts: reset and preparation.

In the reset part we rest the system to a fixed initial state  $\rho_i$ , which has to be unitarily equivalent to  $\bar{\rho}$ . So the system's equilibrium state is not considered because it has different spectra with that of  $\bar{\rho}$ . Although there are many candidates, we choose  $\rho_i \propto \sigma_z^2$  for convenience of observation and design a corresponding initialization procedure, see Fig. 2(b). First, we apply a continuous wave (cw) on the proton channel. Because of the steady state hetero-nuclear Overhauser effect (NOE) [26], provided that the cw irradiation is sufficiently long and strong, then the system will be driven asymptotically into a steady state  $\rho_{ss}$  of the form:  $\rho_{ss} = \sum_{k=1}^4 \epsilon_{ss}^k \sigma_z^k$ , that is, the protons are saturated. In experiment, the irradiation is set to be 10 s of duration and 2500 Hz of magnitude. As expected we see the establishment of the steady state, in which only the carbons' polarizations are left, but with enhanced bias compared to the equilibrium state. For example, the boost factor of  $\text{C}_2$  is about 1.8.

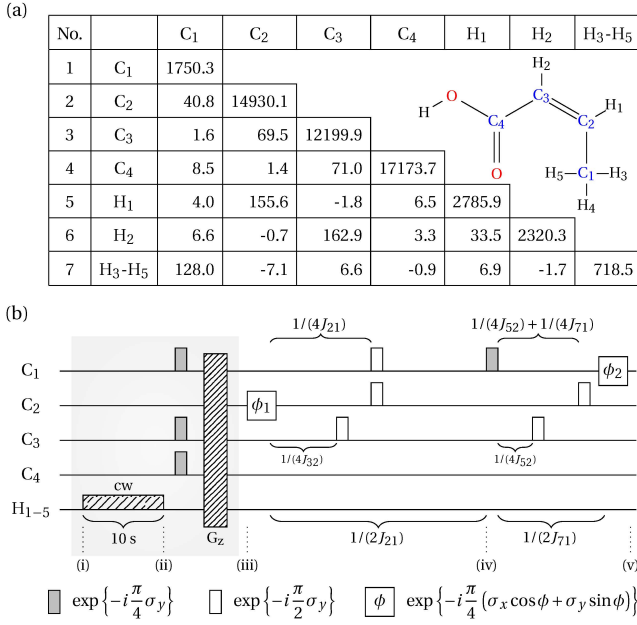


FIG. 2: (a) Crotonic acid molecular diagram and its parameters (all in Hz). In the table, diagonal elements give chemical shifts with respect to the base frequency for carbon and proton transmitters; off-diagonal elements give  $J$  coupling terms. (b) Pulse sequence scheme. The grey part is to reset the system back into  $\rho_i$ , and the preparation part is an approximate circuit (cw: continuous wave;  $G_z$ : gradient pulse along  $z$  axis;  $\phi_1 = -18^\circ$  and  $\phi_2 = 82^\circ$ ) meant for  $\rho_i \rightarrow \bar{\rho}$ . The states at various steps of the circuit are respectively: (i) final state of last experiment; (ii)  $\rho_{ss} = \sum_{k=1}^4 \epsilon_{ss}^k \sigma_z^k$ ; (iii)  $\rho_i = \sigma_z^2$ , here we rescaled  $\epsilon_{ss}$  as 1; (iv)  $-0.3090 \times \sigma_z^1 \sigma_z^2 \sigma_z^3 + 0.9511 \times \sigma_z^1 \sigma_y^2 \sigma_z^3$ ; (v)  $0.9824 \times \sigma_z^1 \sigma_z^2 \sigma_z^3 \sigma_z^5 \sigma_z^7 \sigma_z^8 \sigma_z^9$ .

Next, we retain just the signal of  $C_2$  by first rotate the polarizations of other carbons to the transverse plane and then destroy them with  $z$  axis gradient field.

The preparation part aims at steering  $\rho_i$  towards  $\bar{\rho}$ . To give a good initial control guess to accelerate convergence, we designed an approximate preparation circuit, see Fig. 2(b). The approximate circuit is constructed based on a simplified system Hamiltonian which ignores the small couplings and the small differences between large couplings of the original Hamiltonian. If we turn back to the original Hamiltonian, the circuit generates a final state that deviates  $\bar{\rho}$  only slightly:  $f \approx 0.9824$ . Moreover, the circuit length is 16.36 ms, much shorter than system's relaxation time, so the preparation stage can be taken as unitary. The rotational gates are implemented using Gaussian shaped selective pulses, each has step length  $\tau = 20 \mu s$  but with a different pulse-width. Excluding the free evolutions, we have in total  $2 \times 108$  non-zero pulse parameters to optimize. We have employed a compilation procedure [27, 28] to systematically reduce the errors that come in when the ideal rotational operations are implemented through soft selective pulses, yet  $f$  still drops severely. Therefore, some extent of pulse

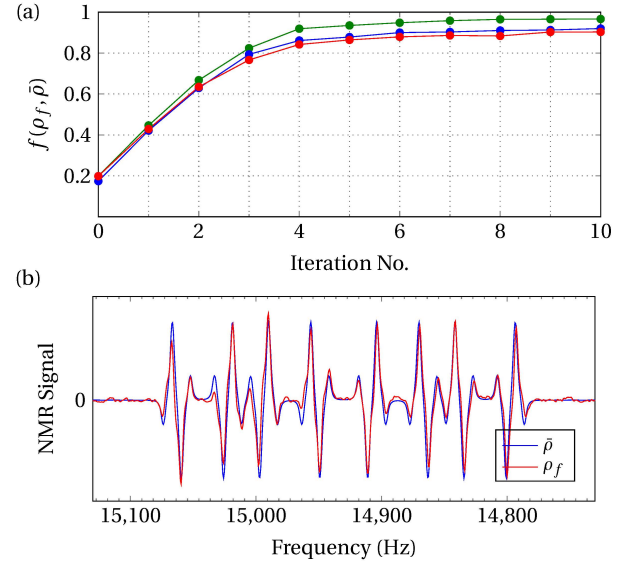


FIG. 3: Experimental results of our quantum oracle machine scheme. (a) GRAPE on our nine-spin system. Let  $u_c$  and  $u_o$  be the controls obtained by searching on a classical computer and on the oracle respectively. The data indicate:  $f(u_c)$  (green); measured  $f(u_o)$  (blue); simulated  $f(u_o)$  (red). (b) NMR spectrum of  $\rho_f$  after 10 times of iteration under the observation of  $C_2$ . The simulated ideal spectrum for target state  $\bar{\rho}$  is rescaled for comparison with experimental signal.

optimization is necessary.

We add a small amount of random disturbances to the above constructed selective pulse network. The purpose of doing so is to start the oracle iteration from a relatively low-quality control and hence to witness a more noticeable rising of  $f$ . We have demonstrated the query action on the sample for 10 rounds, each takes time cost about 4.8 h. Fig. 3 shows the experimental results, from which we see clearly that the oracle's output effectively improves the performance of the control field. Because that measurement inaccuracies induce errors in gradient estimation, it is as expected that some degree of deviation of the experimental growth of  $f$  from that performed on a classical computer appears. Therefore, the important challenge left open is to understand quantitatively how measurement inaccuracies affect the convergence.

*Discussion.*—From the control theory perspective, the apparatus in our experiment, including a control input generator, a sample of molecules and a measurement device, interact as a closed learning loop. In each cycle of the loop, the fitness information learned from the sample directs the optimization to achieve a given control objective. Such strategy has the advantage of reliability and robustness. Learning algorithm is the crucial ingredient, and most previous studies rely on stochastic searching strategies such as evolutionary algorithms [24, 29]. We here show that the greedy algorithm GRAPE can also be incorporated into closed loop control model. There exist



many related variants of GRAPE, among them conjugated gradient [30], monotonic convergent [31], to name a few. It would be interesting to find out whether they can be treated analogously.

Future work will also examine the computational side of the quantum simulator based oracle machine solver for quantum optimal control. NMR is an excellent platform on which to test various quantum control methods, but for our scheme its drawback is the relatively long reset (relaxation) time. It can be envisioned that on some other quantum information processing candidate systems that are with much shorter operation time and relaxation time [2], the oracle searching may get several orders of magnitude faster. We expect the methodology developed in this work can promote studies of scalable quantum controls on larger quantum systems.

This work is supported by the National Basic Research Program of China (973 Program, Grant No. 2014CB921403), the National Key Research and Development Program (Grant No. 2016YFA0301201), the Foundation for Innovative Research Groups of the National Natural Science Foundation of China (Grant No. 11421063), the Major Program of the National Natural Science Foundation of China (Grant No. 11534002), the State Key Development Program for Basic Research of China (Grant Nos. 2014CB848700 and 2013CB921800), the National Science Fund for Distinguished Young Scholars (Grant No. 11425523), and the National Natural Science Foundation of China (Grant No. 11375167).

---

\* Electronic address: [lijunwu@mail.ustc.edu.cn](mailto:lijunwu@mail.ustc.edu.cn)

† Electronic address: [xhpeng@ustc.edu.cn](mailto:xhpeng@ustc.edu.cn)

- [1] M. A. Nielsen and I. L. Chuang, *Quantum Computation and Quantum Information* (Cambridge University Press, Cambridge, 2000).
- [2] T. D. Ladd, F. Jelezko, R. Laflamme, Y. Nakamura, C. Monroe, and J. L. O'Brien, *Nature* (London) **464**, 45 (2010).
- [3] A. M. Childs and W. van Dam, *Rev. Mod. Phys.* **82**, 1 (2010).
- [4] J. I. Cirac and P. Zoller, *Nat. Phys.* **8**, 264 (2012).
- [5] R. P. Feynman, *Int. J. Theor. Phys.* **21**, 467 (1982).
- [6] A. W. Harrow, A. Hassidim, and S. Lloyd, *Phys. Rev. Lett.* **103**, 150502 (2009).
- [7] A. M. Childs, *Nat. Phys.* **5**, 861 (2009).
- [8] G. A. Álvarez, D. Suter, and R. Kaiser, *Science*, **349**, 846 (2015).
- [9] B. P. Lanyon *et al.*, *Nat. Chem.* **2**, 106 (2010).
- [10] P. J. J. O'Malley *et al.*, *Phys. Rev. X* **6**, 031007 (2016).
- [11] N. Wiebe, C. Granade, C. Ferrie, and D. G. Cory, *Phys. Rev. Lett.* **112**, 190501 (2014).
- [12] C. Brif, R. Chakrabarti, and H. Rabitz, *New J. Phys.* **12**, 075008 (2010).
- [13] H. J. Hogben, M. Krzystyniak, G. T. P. Charnock, P. J. Hore, and I. Kuprov, *J. Magn. Reson.* **208**, 179 (2011).
- [14] N. Khaneja *et al.*, *J. Magn. Reson.* **172**, 296 (2005).
- [15] A. M. Turing, *Proc. London Math. Soc.* **45**, 161 (1939).
- [16] E. J. Beggs, J. F. Costa, and J. V. Tucker, *Phil. Trans. R. Soc. A* **370**, 3359 (2012).
- [17] O. Goldreich, *Computational Complexity: A Conceptual Perspective* (Cambridge University Press, Cambridge, England, 2008).
- [18] S. Lloyd, *Science* **273**, 1073 (1996).
- [19] N. Khaneja, R. Brockett, and S. J. Glaser, *Phys. Rev. A* **63**, 032308 (2001).
- [20] A. Carlini, A. Hosoya, T. Koike, and Y. Okudaira, *Phys. Rev. A* **75**, 042308 (2007).
- [21] A. S. Nemirovski and D. B. Yudin, *Problem Complexity and Method Efficiency in Optimization* (Wiley, New York, 1983).
- [22] Y. Nesterov, *Introductory Lectures on Convex Optimization: Basic Course*. (Springer-Verlag, 2004).
- [23] A. N. Pechen and D. J. Tannor, *Phys. Rev. Lett.* **106**, 120402 (2011).
- [24] H. Rabitz, R. de Vivie-Riedle, M. Motzkus, K. Kompa, *Science* **288**, 824 (2000).
- [25] O. W. Sørensen, G. W. Eich, M. H. Levitt, G. Bodenhausen, and R. R. Ernst, *Prog. Nucl. Magn. Reson. Spectrosc.* **16**, 163 (1983).
- [26] M. H. Levitt, *Spin Dynamics: Basics of Nuclear Magnetic Resonance* (John Wiley & Sons Ltd, England, 2008).
- [27] C. A. Ryan, C. Negrevergne, M. Laforest, E. Knill, and R. Laflamme, *Phys. Rev. A* **78**, 012328 (2008).
- [28] J. Li, J. Cui, R. Laflamme, and X. Peng, *Phys. Rev. A* **94**, 032316 (2016).
- [29] R. S. Judson and H. Rabitz, *Phys. Rev. Lett.* **68**, 1500 (1992).
- [30] A. Borzì, J. Salomon, and S. Volkwein, *J. Comput. Appl. Math.* **216**, 170 (2008).
- [31] I. I. Maximov, Z. Tošner, and N. C. Nielsen, *J. Chem. Phys.* **128**, 184505 (2008); I. I. Maximov, J. Salomon, G. Turinici, and N. C. Nielsen, *J. Chem. Phys.* **132**, 084107 (2010).